ISSN 0036-0244, Russian Journal of Physical Chemistry, 2006, Vol. 80, Suppl. 1, pp. S55–S62. © Pleiades Publishing, Inc., 2006.

STRUCTURE OF CHEMICAL COMPOUNDS, INCLUDING CONDENSED MEDIA

Monte Carlo Simulation Study of Melittin: Protein Folding and Temperature Dependence[1]

M. Monajjemi[a], S. Ketabi[b], and A. Amiri[c]

[a] *Department, Islamic Azad University, Science and Research Campus, Hesarak, Tehran, P.O. Box 14155-775 Iran*
E-mail: m_monajjemi@yahoo.com

[b] *Department of Chemistry, East Tehran Campus (Ghiam Dasht) Islamic Azad, University, Tehran, Iran*

[c] *Department of Chemistry, Central Tehran Campus, Islamic Azad University, Tehran, Iran*

Received December 9, 2005

Abstract—The tetramerization of melittin, a 26-amino-acid peptide, is considered as a model for protein folding. The Monte Carlo simulation was used to study the folding arrangement of melittin, and the results are compared with the experiment. An acceptance rate of 50% for new configurations is achieved by using ranges of ±0.001 Å for the translations and ±15°C for the rotations. Around 311 K, the folded structure of the protein has the greatest stability; the range from –40 to –80 shows the best φ angles for melittin. The final optimized structure of melittin strongly depends on the temperature. The melittin tetramer is found to have a temperature of maximum stability ranging from 35.5 to 43°C.

DOI: 10.1134/S0036024406130103

INTRODUCTION

Melittin is a small polypeptide that consists of 26 amino acids ($C_{133}H_{229}N_{39}O_{31}$). It contains a single essential fluorophore, tryptophane [1]. When completely folded it forms symmetrical tetramers [2, 3]. Its structure has been determined to a high degree of resolution by X-ray crystallography [2] and NMR spectroscopy. The NMR structures have been determined in detergent micelles [4] and in nonpolar solvent [5], in which the protein is present as a monomeric form while crystals grow from concentrated aqueous salt solutions in which melittin molecules form closely associated tetramers through hydrophobic contacts [2]. These studies indicate that melittin adopts very similar ahelical conformations in the very different environments.

Melittin originates in honeybee (*Apis mellifera*) venom, of which it composes 50% of the dry weight. In a neutral situation, melittin has a net charge of +5 (4 from the leu amino acids and 1 from the N-terminus). This charge inhibits the formation of any secondary structure under neutral conditions. It is attractive to assume that proteins in different classes might display significantly different presentations in their folding pathways. Melittin is usually a random coil monomer, but when basic conditions or other effects shield the charge, melittin forms 2α-helices at an angle of 120° to each other. This angle gives amino acids 11–13 some helical character. Amino acids 5–11 and 16–24 have the most helical natures [6, 7]. Four of these α-helical monomers can then form a tetramer. That melittin has one tryptophane amino acid (Trp19) is another argument for the use of melittin as a folding model. This is because Trp19 is the only amino acid in melittin that fluoresces and its spectrum is dependent on the polarity of the solvent. The more structured it is, the more the Trp19 is shielded from the aqueous medium [8].

The melittin occupation depends strongly on the solvent and the temperature. Increasing the concentration of melittin promotes a helical state. The state in which melittin exists depends strongly on the temperature. When using circular dichroism, both hot and cold denaturations are found. But the temperature of the maximum helicity depends markedly on the solvent used and on the melittin concentration. The α-helical position has its steadiest pattern between 35.5 and 43°C, depending on pH [9]. Not many thermodynamical studies of melittin have been performed to date. The folding process of melittin can be divided into two different processes: α-helix configuration and tetramerization of single melittin molecules. However, these processes depend on each other and, under steady-state conditions, are thought to occur all at once [10]. The melittin folding equilibrium depends on many variables, and we are mostly concerned with its temperature dependence, as we want to use the system for dynamical studies also. Thus far, the temperature dependence of the folding equilibrium has been calculated by a number of different spectroscopic techniques: NMR [6], circular dichroism [7, 11], fluorescence [12], and fluorescence polarization [13]. Smoluch and et al. [14] have studied the temperature dependence of the melittin folding equilibrium by means of fluorescence spectroscopy.

[1] The text was submitted by the authors in English.

A great deal of information is currently known regarding the general principles of the folding and structural stability of soluble proteins [15, 16]. Some general principles are beginning to emerge [17–20], but the amount of thermodynamic data is quite limited, due principally to the experimental difficulties caused by their insolubility in water in both folded and unfolded forms.

A common approach to the thermodynamic stability of proteins is to study the energetics of the folding/unfolding process [21] induced by heat [22] or denaturants [23]. In this approach, which requires that the folding/unfolding reaction be reversible, as discussed by Haltia and Freire [24], the main difficulty is that membrane proteins resist complete denaturation because of the great stability of the transmembrane secondary structure elements within the membrane. The denaturizing that does occur is frequently irreversible and arises mainly from the dissociation of multimers, subunits, and secondary structure elements and the unfolding of extra membrane domains. The stability of the individual secondary structure elements, usually K-helices, is exposed by the great amount of the secondary structure (determined by circular dichroism) that remains after denaturation. This residual structure within the membrane phase (bilayers or micelles) indicates the resistance of secondary structure elements to adsorption and/or unfolding under a denaturing situation.

It has been shown that [25], while melittin at micro molar concentrations is unfolded under conditions of low salt concentration at neutral pH, it transforms into an α-helical tetramer under high-salt conditions or alkaline pH. Generally, statistical treatments of protein conformations have considered the interdependence of the backbone torsion ψ and φ angles neighboring the peptide bond (Ramachandran plots) and neglected higher order interdependences between bond dihedral angles. Systematic analyses of ψ and φ angles for different types of amino acids lead to resemblance coefficients between amino acid pairs, which are practical in estimating the structural effects of amino acid substitutions and providing an efficient scoring scheme for sequence alignments [26]. On the other hand, common secondary structure motifs, such as α-helices and β-sheets, result from the repetition of well-defined rotations along the main chain. Turns also constitute units that are distinguishable by their particular dihedral angle sequences. Applications such as protein folding require an understanding of the conformational space of these macromolecules.

Biomolecules with the common all-atom force fields have rugged energy landscapes and multiple time scales that both limit the small time step of molecular dynamics (MD) and require the integration of many time steps to sufficiently sample the slow molecular modes. This is exacerbated by trappings in local minima to try to overcome these problems with some techniques, such as Monte Carlo simulation. We have attempted to use the Monte Carlo simulation method when the goal is single temperature canonical sampling. This turns to suggest other simulation strategies, such as Hamiltonian exchange [27] and resolution exchange [28]. Rathore and de Pablo [29] have also performed Monte Carlo simulation through a random walk in energy space to study random coil–helix and random coil–beta sheet transitions in model proteins. They employed a cubic lattice model, and have shown that the method is able to fold long polypeptides reproducibly.

MOLECULAR MECHANICS FORCE FIELD

Calculations were performed with the Charmm simulation program [30], in which an empirical energy function that contains terms for both internal and external interactions was used. The energy function has the form

$$E(R)_{\text{total}} = E(R)_{\text{internal}} + E(R)_{\text{external}},$$

$$E_{\text{internal}} = \sum_{\text{bonds}} K_b(b - b_0)^2 + \sum_{UB} K_{UB}(S - S_0)^2$$

$$+ \sum_{\text{angles}} K_\theta(\theta - \theta_0)^2 + \sum_{\text{dihedras}} K_\chi(1 + \cos(n\chi - \delta))$$

$$+ \sum_{\text{improper}} K_{\text{imp}}(\varphi - \varphi_0)^2,$$

$$E(R)_{\text{external}}$$

$$= \sum_{\substack{\text{nonbed} \\ \text{atompairs}}} \left(\varepsilon_{ij} \left[\left(\frac{R_{\min ij}}{r_{ij}} \right)^{12} - \left(\frac{R_{\min ij}}{r_{ij}} \right)^{6} \right] + \frac{q_i q_j e^2}{r_{ij}} \right),$$

where K, K_{UB}, K_θ, K_χ and K_{imp} are the bond, Urey–Bradley, angle, dihedral angle, and improper dihedral angle force constants, respectively, and b, S, θ, χ and φ are the bond length, Urey–Bradley 1,3-distance, bond angle, dihedral angle, and improper torsion angle, respectively, with the subscript zero representing the equilibrium values for the individual terms. From 6 to 12 Coulomb and Lennard-Jones terms contribute to the nonbonded interactions. ε is the Lennard-Jones well depth, $R_{\min}$ is the distance at the Lennard-Jones minimum, and q_i is the partial atomic charge. The Lennard-Jones parameters between pairs of different atoms are obtained from the Lorentz–Bethelodt combination rules.

MONTE CARLO PROCEDURE

Monte Carlo statistical mechanical simulations were carried out in a standard manner using the

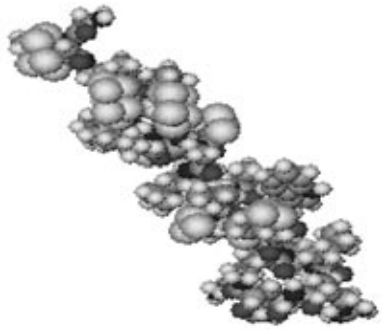

Fig. 1. Resultant structure of melittin.

Metropolis sampling technique [31] in a canonical (*T*, *V*, *N*) ensemble. In Monte Carlo simulations, making random structural changes to the internal degrees of freedom and subsequently accepting or rejecting them based on the Metropolis criterion at generating new molecular configurations of the system. One of the potential advantages of this is that the simulation trajectory is a Markov chain of configurations that explores phase space in a time-independent manner, thereby formulating an equilibrium statistical mechanical representation of the system. With sufficient sampling, this can be used to derive a wide variety of thermodynamic parameters.

Minimizing the peptide has been divided to two sections: the main chain and side chain of peptide. In the backbone moves, one unit was randomly selected and the backbone (ψ, φ) torsion angles are changed. The maximum of the moves have been chosen ±15°. The resulting conformation has been minimized and accepted or rejected according to the Metropolis criterion.

The second stage of optimization has been done with moves in the side chain. For the Monte Carlo simulation of the side chain of melittin, two types of move have been considered. One of the four hundred and thirty-three atoms of melittin is first randomly chosen and then moves in the maximum range of ±0.001 Å randomly. The second type of move was the rotation of peptide side chain torsions. New configurations were achieved by using ranges of ±50°. Periodic boundary conditions were employed in computation. A spherical cut-off for the potential of 13 Å has been used for nonbonded interactions. The system is thoroughly equilibrated by using several hundreds-of-thousand configurations. Each run consisted of 10^5–10^6 attempted moves. Every calculation was extended to include as many configurations as were necessary to reduce the statistical error to the level at which calculated energy differences have quantitative significance. We have done the computations in the different dr_{max} (maximum range of displacement of atoms) and $d\theta_{max}$ (maximum range of rotations) ranges to find the optimum value of dr_{max}. All the simulations were carried out in the temperature range of 303–314 K.

RESULTS AND DISCUSSION

Protein folding involves a complex molecular recognition process that depends on the cooperative action of many interactions. It is a heterogeneous process, and the net stability is the result of relations between entropic and enthalpic contributions. The folding mechanism can be described using the manner in which the protein finds its native structure within a short period (seconds or minutes) of time. Many diseases are caused by misfolded proteins (e.g., cancer). In the improvement in methodology for statistical prediction of protein structures, the inventors of different methods

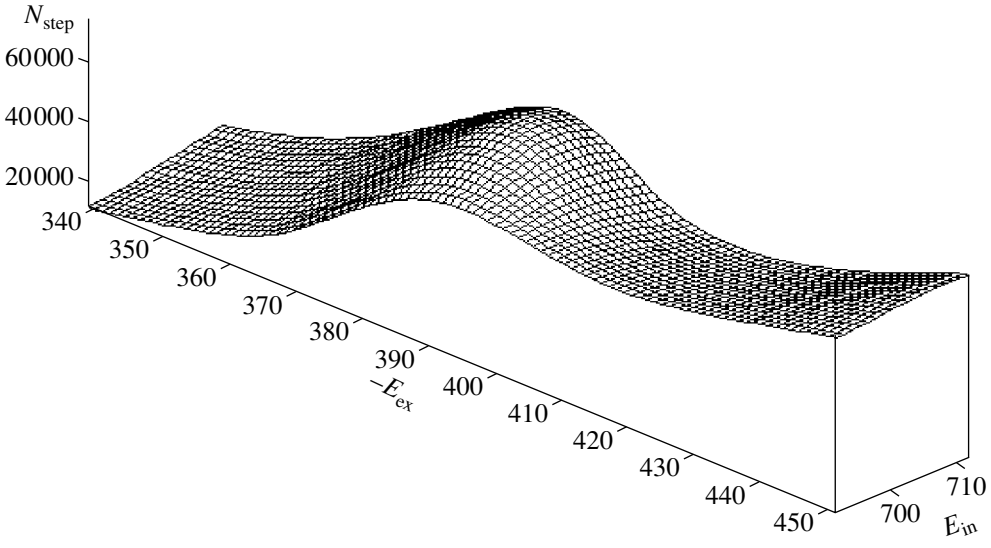

Fig. 2. Internal and external energies vs. N_{step}.

Table 1. Internal and external energies at different displacements at 300 K

dr, Å	E_{total}	$E_{internal}$					$E_{external}$	
		E_{bonds}	E_{angles}	$E_{urey\text{-}b}$	$E_{dihedrals}$	$E_{impropers}$	$-E_{vdw}$	$-E_{elec}$
0.001	356.03	108.40	396.89	35.56	140.705	13.014	40.38	298.16
0.010	348.14	125.31	384.35	35.80	139.01	15.22	48.33	303.22
0.020	369.08	145.90	373.92	32.33	155.17	15.80	45.06	308.97
0.050	319.44	151.87	323.22	31.50	154.79	12.49	50.09	304.34
0.080	286.54	131.98	323.56	33.05	144.83	13.55	32.41	328.02
0.100	268.32	157.82	296.07	36.64	152.07	10.84	46.13	339.00
0.150	253.21	169.45	272.87	34.18	141.10	11.56	34.22	341.72
0.200	233.58	151.05	258.27	30.36	160.55	16.75	21.73	361.68

Note: All of the energies are in kcal/mol.

Table 2. Internal and external energies at different rotation angles at 300 K

$d\theta$, deg	E_{total}	$E_{internal}$					$E_{external}$	
		E_{bonds}	E_{angles}	$E_{urey\text{-}b}$	$E_{dihedrals}$	$E_{impropers}$	$-E_{vdw}$	$-E_{elec}$
35	326.95	107.09	396.42	35.36	143.58	13.26	50.96	317.80
40	332.27	108.83	395.24	35.47	142.00	13.16	48.36	314.07
45	350.44	108.23	396.78	35.47	138.24	13.19	43.57	297.90
50	356.03	108.40	396.89	35.56	140.70	13.01	40.38	298.16
55	335.18	106.94	396.93	35.53	153.95	13.35	45.62	325.90
60	356.57	107.48	396.88	35.59	156.36	13.20	47.44	305.50

Note: All of the energies are in kcal/mol.

Table 3. Internal and external energies in different NSTEPs and the total number of MC steps, at 300 K

N_{step}	E_{total}	$E_{internal}$					$E_{external}$	
		E_{bonds}	E_{angles}	$E_{urey\text{-}b}$	$E_{dihedrals}$	$E_{impropers}$	$-E_{vdw}$	$-E_{elec}$
10000	356.03	108.40	396.89	35.56	140.70	13.01	40.38	298.16
20000	324.71	107.32	397.43	35.56	138.44	13.26	44.14	323.15
40000	323.15	109.54	397.06	35.73	154.60	14.18	48.78	357.34
50000	290.35	108.98	397.12	35.65	156.82	13.67	47.85	374.04
60000	273.19	109.79	399.87	35.78	152.43	13.27	57.83	380.13
80000	257.95	111.93	396.46	35.87	150.74	14.03	50.40	400.69
100000	254.22	108.07	394.12	35.92	153.81	14.19	30.26	421.64

Note: All of the energies are in kcal/mol.

Table 4. Total, internal, and external energies at different temperatures

T, K	E_{total}	$E_{internal}$					$E_{external}$	
		E_{bonds}	E_{angles}	$E_{urey\text{-}b}$	$E_{dihedrals}$	$E_{impropers}$	$-E_{vdw}$	$-E_{elec}$
303	344.03	107.45	397.08	35.41	145.11	13.28	49.42	304.88
304	375.83	107.79	396.93	35.37	148.08	13.04	40.89	284.49
305	340.91	107.29	396.80	35.46	149.27	13.24	53.87	307.28
306	341.29	107.18	396.76	35.47	145.11	13.21	52.22	304.22
307	338.32	107.36	396.59	35.47	145.75	13.16	46.52	313.49
308	338.32	107.36	396.59	35.47	145.75	13.16	46.52	313.49
309	338.32	107.36	396.60	35.47	145.74	13.16	46.52	313.49
310	338.32	107.36	396.60	35.47	145.74	13.16	46.52	313.49
311	334.04	107.35	396.59	35.44	140.26	13.13	53.48	305.25
312	338.01	107.93	396.33	35.45	156.12	13.21	44.25	326.77
313	338.01	107.97	396.33	35.45	156.12	13.21	44.25	326.77
314	344.52	107.69	396.33	35.48	147.84	13.23	54.49	301.57

Note: All of the energies are in kcal/mol.

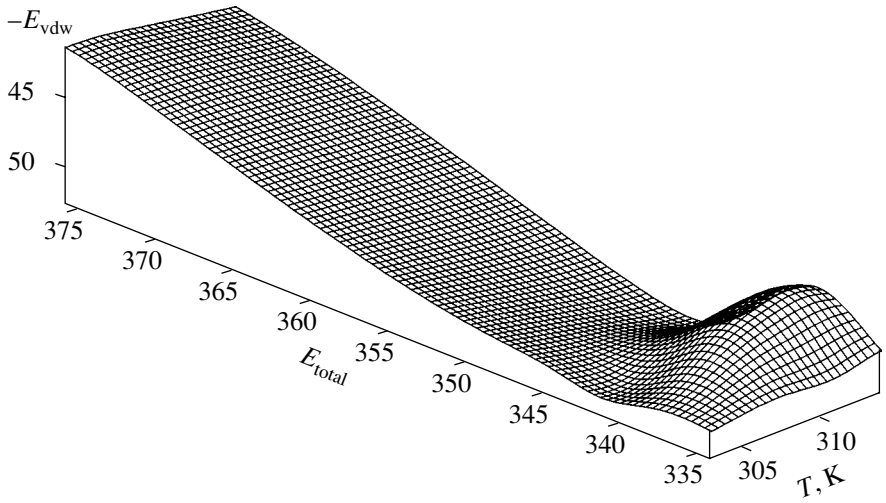

Fig. 3. Total and Van der Waals energies vs. temperature.

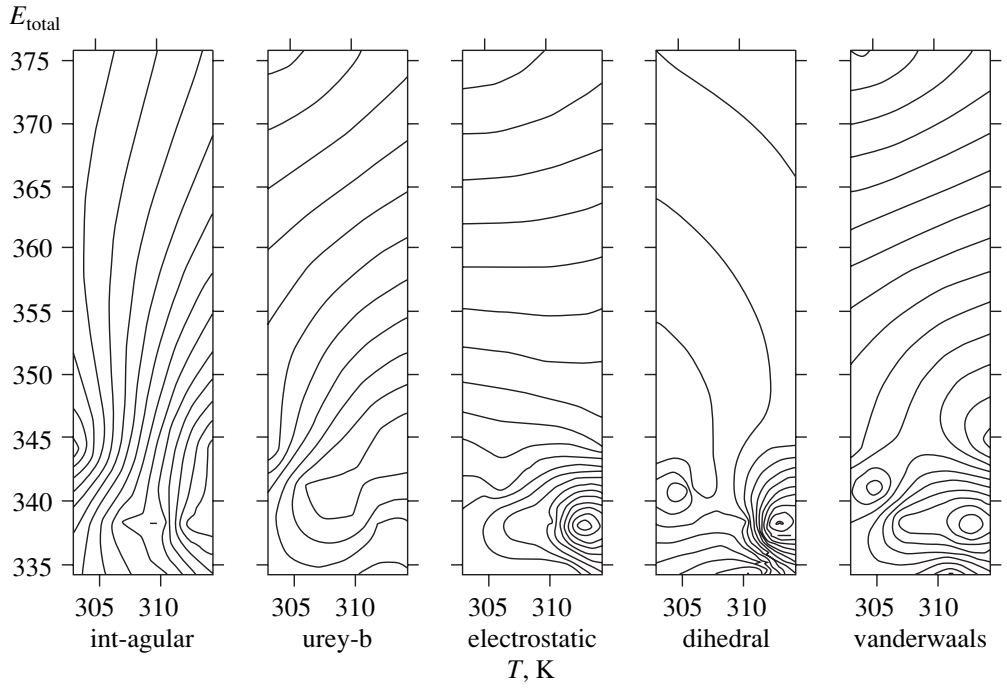

Fig. 4. Contour diagram of van der Waals energy, total electrostatic energy, dihedral energy, internal angular energy, and internal Urey Bradley energy vs. temperature and total energy.

usually have selected different sets of proteins to test the predicted results. Therefore, it is hard to make a fair comparison using the results they have reported. A Monte Carlo simulation method is proposed to establish an objective criterion to measure the accuracy of prediction for the protein folding type. Such an objective accuracy actually corresponds to the asymptotic limit generated during the Monte Carlo simulation process.

We have studied the folded structure of melittin by the Monte Carlo simulation. For the melittin folded molecule, noticeable changes with temperature have been observed. The resultant structure of melittin is shown in Fig. 1. We have used different values for the displacements in different NSTEPs to find the best condition for optimizing the melittin structure. Internal and external energies in different displacements, rotations, and NSTEPs (the total

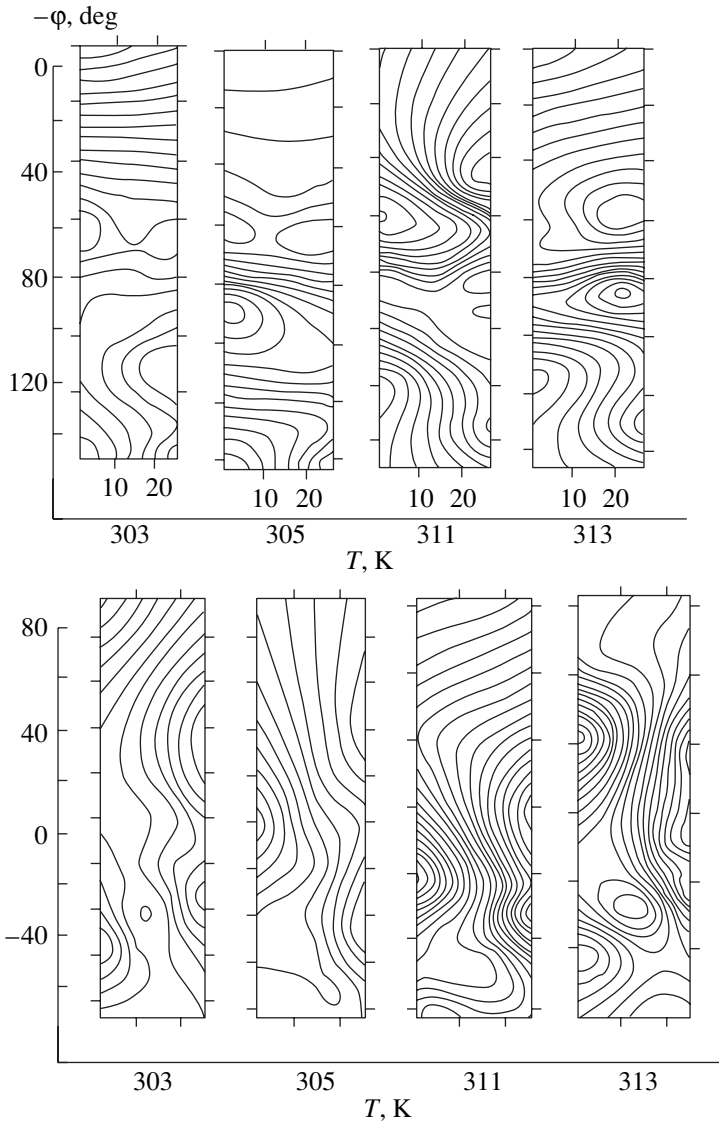

Fig. 5. Angles ψ and φ vs. temperature.

number of MC steps) at 300 K have been included in Tables 1–3 respectively.

An increasing or decreasing the temperature from the temperature of maximum stability ranging from 35.5 to 43°C destabilizes the Melittin tetramer.

As is shown in Table 1, E_{bond} has the minimum value in the 0.001 Å displacement; also, almost 50% of the configurations shown have been accepted [32]. In Table 2, internal and external energies in different rotations have been shown and as a maximum range of ±50° has been chosen, 50% of the configurations have been accepted. Table 3 includes the internal and external energies versus the total number of MC steps. In Fig. 2, the internal and external energies versus NSTEP are presented. Temperature-induced changes in the Monte Carlo optimization of the melittin folded molecule have been observed.

In Table 4, the total, internal, and external energies at different temperatures are shown. The temperature dependencies exhibited in the three-dimensional diagrams, in which the temperature is plotted against the total energy, van der Waals energy, total electrostatic energy, dihedral energy, internal angular energy, and internal Urey–Bradley energy are consistent in their results. As an example in Fig. 3, a three-dimensional graph consisting of the total and van der Waals energies versus the temperature for the folded melittin is presented. It is specified that, at 304.76 K, the total energy is 341.22 kcal/mol and the external van der Waals energy is the lowest one (–53.44 kcal/mol).

The variations of total energies and electrostatic energies against different temperatures shows that, at 312.7 K, the total energy is 338.17 kcal/mol and the total electrostatic energy is minimal (–326.59 kcal/mol). The

Table 5. Energetic parameters at different temperatures

T, K	E_{total}	$E_{internal}$					$E_{external}$	
		E_{bonds}	E_{angles}	$E_{urey\text{-}b}$	$E_{dihedrals}$	$E_{impropers}$	$-E_{vdw}$	$-E_{elec}$
303	344.03	107.45	397.08	35.41	145.11	13.28	49.42	304.88
304	375.83	107.79	396.93	35.37	148.08	13.04	40.89	284.49
305	340.91	107.29	396.80	35.46	149.27	13.24	53.87	307.28
306	341.29	107.18	396.76	35.47	145.11	13.21	52.22	304.22
307	338.32	107.36	396.59	35.47	145.75	13.16	46.52	313.49
308	338.32	107.36	396.59	35.47	145.75	13.16	46.52	313.49
309	338.32	107.36	396.60	35.47	145.74	13.16	46.52	313.49
310	338.32	107.36	396.60	35.47	145.74	13.16	46.52	313.49
311	334.04	107.35	396.59	35.44	140.26	13.13	53.48	305.25
312	338.01	107.92	396.33	35.45	156.12	13.21	44.25	326.77
313	338.01	107.97	396.33	35.45	156.12	13.21	44.25	326.77
314	344.52	107.70	396.33	35.48	147.84	13.24	54.49	301.57

variation of total energies and dihedral energies against different temperatures specifies that at 310.04 K the total energy is 334.04 kcal/mol and the total electrostatic energy is minimal (140.90 kcal/mol). The variation of total energies and internal angular energies against different temperature means that, at 307.4 K, the total energy is 334.04 kcal/mol and the total electrostatic energy is minimal (396.65 kcal/mol).

In Fig. 4, van der Waals energy, total electrostatic energy, dihedral energy, internal angular energy, and internal Urey–Bradley energy are plotted as contour diagrams against temperature and the total energy. Consequently, it is specified that, near 36.5°C, the internal and external energies are probably minimal and the folded structure is in its most stable form. Calculations at different temperatures have been done to predict the effect of temperature on the stability of protein. The energy parameters at different temperatures have been included in Table 5; at around biological temperature, melittin has a minimum total energy and so, at this temperature, it has the most stably folded structure. Where degenerate lines are pressed, the stability of the structure will increase. Therefore, at around 311 K, the folded structure of the protein has the most stability. Thus, the range of from –40 to –80 shows the best φ angles for melittin. In Fig. 5, contour diagrams of ψ and φ angles in different temperatures are reported.

CONCLUSIONS

The purpose of fold assignment and relative modeling is to assign each novel genome sequence to the identified protein fold or structure that it most directly resembles using computational Monte Carlo methods. These calculations provide visualization of the relative importance of various forces affecting the stability of melittin in the folded structure and may provide a standard arrangement for future tests of computated energies on this simple protein system.

REFERENCES

1. S. C. Quay and C. C. Condie, Biochemistry **22**, 659 (1983).
2. T. C. Terwillinger and D. Eisenberg, J. Biol. Chem. **257**, 6010 (1982).
3. T. C. Terwillinger and D. Eisenberg, J. Biol. Chem. **257**, 6016 (1982).
4. F. Inagaki, I. Shimada, K. Kawaguchi, et al., Biochemistry **28**, 5985 (1989).
5. R. Bazzo, M. J. Tappin, A. Pastore, et al., Eur. J. Biochem. **173**, 139 (1988).
6. M. Iwadate, T. Asakura, and M. P. Williamson, Eur. J. Biochem. **257**, 479 (1998).
7. K. Ramalingam, S. Aimoto, and J. Bello, Biopolymers **32**, 981 (1992).
8. M. van Veen, G. N. Georgiou, A. F. Drake, and R. J. Cherry, Biochem. J. **305**, 7857 (1995).
9. Y. Sakakibara, M. Brown, R. Hughey, et al., Nucleic Acids Res. **22**, 5112 (1994).
10. E. Habermann and J. Jentsch, Physiol. Chem. **348**, 37 (1967).
11. W. Wilcox and D. Eisenberg, Protein Sci. **1**, 641 (1992).
12. A. P. Demchenko, A. S. Ladokhin, E. G. Kostrzhewskaya, and T. L. Dibrova, Mol. Biol. **21**, 663 (1987).
13. J. F. Faucon, J. Dufourcq, and C. Lussan, FEBS Lett. **102**, 187 (1979).
14. M. Smoluch, M. Gorseling, C. Gooijer, and G. Zwan, J. Fluoresc. **14** (1), 37 (2004).
15. K.A. Dill, Biochemistry **29**, 71337 (1990).

16. T. E. Creighton, *Protein Folding* (W. H. Freeman, New York, 1992), pp. 1–547.
17. J.-L. Popot, Curr. Opin. Struct. Biol. **3**, 532 (1993).
18. S.H. White, W.C. Wimley, Curr. Opin. Struct. Biol. **4**, 79 (1994).
19. *Membrane Protein Structure: Experimental Approaches*, Ed. by S. H. White (Oxford Univ., Oxford, 1994), pp. 1–359.
20. D. C. Rees, A. J. Chirino, K.-H. Kim, and H. Komiya, in *Membrane Protein Structure: Experimental Approaches*, Ed. by S. H. White (Oxford Univ., Oxford, 1994), pp. 3–26.
21. F. M. Richards, in *Protein Folding*, Ed. by: T. E. Creighton (W. H. Freeman, New York, 1992), pp. 1–58.
22. P. L. Privalov, in *Protein Folding*, Ed. by: T. E. Creighton (W. H. Freeman, New York, 1992), pp. 83–126.
23. C. N. Pace, Methods Enzymol. **131**, 266 (1986).
24. T. Haltia and E. Freire, Biochim. Biophys. Acta **1241**, 295 (1995).
25. K. Ramalingam, J. Bello, and S. Aimoto, FEBS Lett. **295**, 200 (1991).
26. K. Niefind and D. Schomburg, J. Mol. Biol. **219**, 481 (1991).
27. Y. Sugita, A. Kitao, and Y. Okamoto, J. Chem. Phys. **113**, 6042 (2000).
28. E. Lyman, F. M. Ytreberg, and D. M. Zuckerman, Phys. Rev. Lett. (in press).
29. N. Rathore and J. de Pablo, J. Chem. Phys. **116**, 7225 (2002).
30. B. R. Brooks, R. E. Bruccoleri, B. D. Olafson, et al., J. Comput. Chem. **4**, 187 (1983).
31. N. Metropolis, A. W. Rosenbulth, M. N. Rosenbulth, et al., J. Chem. Phys. **21**, 1087 (1953).
32. P. J. Steinbach, Proteins, p. 6656 (2004).